ELSEVIER

Engineering Analysis with Boundary Elements 28 (2004) 535–545

ENGINEERING ANALYSIS with BOUNDARY ELEMENTS

www.elsevier.com/locate/enganabound

A meshless method for free vibration analysis of circular and rectangular clamped plates using radial basis function

J.T. Chen[a,*], I.L. Chen[b], K.H. Chen[a], Y.T. Lee[a], Y.T. Yeh[a]

[a]*Department of Harbor and River Engineering, National Taiwan Ocean University, P.O. Box 7-59, Keelung 20224, Taiwan, ROC*
[b]*Department of Naval Architecture, National Kaohsiung Institute of Marine Technology, Kaohsiung, Taiwan, ROC*

Received 20 July 2002; revised 3 March 2003; accepted 5 April 2003

Abstract

In this paper, a meshless method for solving the eigenfrequencies of clamped plates using the radial basis function (RBF) is proposed. The coefficients of influence matrices are easily determined by the two-point function. By employing the RBF in the imaginary-part fundamental solution, true eigensolutions instead of spurious one are obtained for plate vibration. In order to obtain the eigenvalues and boundary modes at the same time, singular value decomposition technique is utilized. Two examples, circular and rectangular clamped plates, are demonstrated to see the validity of the present method.

Keywords: Meshless method; Radial basis function; Plate vibration; Clamped boundary; General solution; Imaginary–park fundamental solution

1. Introduction

In numerical methods, mesh generation of a complicated geometry is always time consuming in the stage of model creation for engineers in dealing with the engineering problems by employing the finite difference method (FDM), finite element method (FEM) and boundary element method (BEM). In the last decade, researchers have paid attention to the meshless method without employing the concept of element. The initial idea of meshless method dates back to the smooth particle hydrodynamics (SPH) method for modeling astrophysical phenomena [1]. Several meshless methods have also been reported in the literature, for example, the domain-based methods including the element-free Galerkin method [2], the reproducing kernel method [3], and boundary-based methods including the boundary node method [4], the meshless local Petrov–Galerkin approach [5], the local boundary integral equation method [6], the radial basis function (RBF) approach [7–12], and the boundary knot method (BKM) [13–16].

Integral equations and BEM have been utilized to solve the interior and exterior boundary value problems for a long time. Several approaches, e.g. complex-valued BEM [17,18], dual reciprocity method (DRM) [19], particular integral method [20], multiple reciprocity method (MRM) [21–23], the real-part BEM [24,25] and imaginary-part BEM [26], have been developed for eigenproblems. To solve eigenproblems by using the complex-valued BEM, the influence coefficient matrix would be complex arithmetics [17]. Therefore, Tai and Shaw [27] employed only the real-part kernel to solve the eigenvalue problems and to avoid the complex-valued computation in sacrifice of occurrence of spurious eigenvalues. The computation of the real-part kernel method or the MRM [23,27,28] has some advantages, but it still faces both the singular and hypersingular integrals. To avoid the singular and hypersingular integrals, De Mey [29] used imaginary-part fundamental solution to solve the eigenproblems. At the same time, De Mey also found the spurious eigensolutions but he did not study them analytically. For the dynamic analysis in BEM, the readers can consult Refs. [30–32]. Kang et al. proposed the non-dimensional

* Corresponding author. Tel.: +886-2-24622192-6177; fax: +886-2-24632375.
E-mail address: jtchen@mail.ntou.edu.tw (J.T. Chen).

0955-7997/$ - see front matter © 2003 Elsevier Ltd. All rights reserved.
doi:10.1016/S0955-7997(03)00106-1

dynamic influence function (NDIF) method to solve eigenproblems of membranes [33,34], acoustic cavities [35], and plates [36]. Later, Chen et al. commented that the NDIF method is a special case of imaginary-part BEM after lumping the distribution of density function for membrane vibrations [37], acoustics [38] and plates vibration [39]. Nevertheless, spurious eigensolutions are inherent in the imaginary-part BEM, real-part BEM and MRM. Instead of using the net approach [35], the double-layer potential approach was employed to avoid the occurrence of spurious eigenvalues [38,40]. An extension to three-dimensional (3D) cavities [41] was done. Numerically speaking, the spurious eigensolutions result from the rank deficiency of the coefficient matrix. This implies the fewer number of constraint equations making the solution space larger. Mathematically speaking, the spurious eigensolutions for interior problems and fictitious frequency for exterior problems arise from the same source of "improper approximation of the null space of operator".

In this paper, we will employ the imaginary-part fundamental solution as RBF to solve the plate vibration problems. The main difference between the present formulation and the method of fundamental solution is that we adopt only the imaginary-part fundamental solution instead of employing the complex-valued kernel. In solving the problem numerically, elements are not required and only boundary nodes are necessary. Both the collocation and source points are distributed on the boundary only. Besides, the kernel function is composed of two-point function, which is a kind of RBF. RBF or distant function depends only on the radial distance of the two points, while a two-point function may depend on the normal vectors of the two points. The difference between the present method and the NDIF method will be emphasized in selecting the interpolation bases. The difference between the Chen's method–boundary knot method (BKM) [14] and our paper as well as the NDIF method is that BKM also employs the DRM to handle inhomogeneous source term and has in depth analysis and extensive use of various general solution to 2D and 3D Helmholtz, Laplace, diffusion and convection–diffusion problems as shown in Ref. [16]. The occurrence of spurious eigenvalues will be discussed. For the special case of circular plate, the eigensolutions will be analytically derived in the discrete system by using circulants. In addition, the true eigenvalues for a circular plate will be derived exactly by approaching the discrete system to the continuous system using the eigenspectrum of circulants [42]. By employing the degenerate kernel and Fourier series expansion, the interior modes will be derived analytically. Two examples, circular and rectangular plates subject to clamped boundary conditions, will be demonstrated to see the validity of the present formulation.

2. Meshless formulation using radial basis function of the imaginary-part fundamental solution

The governing equation for a free flexural vibration of a uniform thin plate is written as follows

$$\nabla^4 w(x) = \lambda^4 w(x), \qquad x \in \Omega, \tag{1}$$

where w is the lateral displacement, $\lambda^4 = \omega^2 \rho_0 h/D$, λ is the frequency parameter, ω is the circular frequency, ρ_0 is the surface density, D is the flexural rigidity expressed as $D = Eh^3/12(1-\nu^2)$ in terms of Young's modulus E, the Poisson ratio ν and the plate thickness h, and Ω is the domain of the thin plate.

The radial basis function (RBF) is defined by

$$G(x,s) = \varphi(|s-x|), \tag{2}$$

where x and s are the collocation and source points, respectively. The Euclidean norm $|s-x|$ is referred to as the radial distance between the collocation and source points. The two-point function $(\varphi(|s-x|))$ is called the RBF since it depends on the radial distance between x and s. By considering the imaginary-part fundamental solution $(W(s,x) = \mathrm{Im}\{(\mathrm{i}/8\lambda^2)\times (H_0^{(2)}(\lambda r) + H_0^{(1)}(\mathrm{i}\lambda r))\})$ [43] for the plate vibration. After adopting the imaginary-part kernel, the displacement and slope can be represented by

$$w(x) = \sum_{j=1}^{2N} W(s_j,x)A(s_j) + \sum_{j=1}^{2N} \Theta(s_j,x)B(s_j), \qquad x \in \Omega, \tag{3}$$

$$\theta(x) = \sum_{j=1}^{2N} W'(s_j,x)A(s_j) + \sum_{j=1}^{2N} \Theta'(s_j,x)B(s_j), \qquad x \in \Omega, \tag{4}$$

where $A(s_j)$ and $B(s_j)$ are the generalized unknowns at s_j, $2N$ is the number of source points and the four kernels are

$$W(s,x) = \frac{1}{8\lambda^2}(J_0(\lambda r) + I_0(\lambda r)), \tag{5}$$

$$\Theta(s,x) = \frac{\partial W(s,x)}{\partial n_s} = \frac{1}{8\lambda}\frac{-J_1(\lambda r) + I_1(\lambda r)}{r} y_i n_i, \tag{6}$$

$$W'(s,x) = \frac{\partial W(s,x)}{\partial n_x} = \frac{1}{8\lambda}\frac{J_1(\lambda r) - I_1(\lambda r)}{r} y_i \bar{n}_i, \tag{7}$$

$$\Theta'(s,x) = \frac{\partial^2 W(s,x)}{\partial n_s \partial n_x} = \frac{1}{8\lambda}\left(\frac{-\lambda J_2(\lambda r) y_i y_j n_i \bar{n}_j}{r^2} + \frac{J_1(\lambda r) n_i \bar{n}_i}{r} - \frac{\lambda I_2(\lambda r) y_i y_j n_i \bar{n}_j}{r^2} - \frac{I_1(\lambda r) n_i \bar{n}_i}{r}\right), \tag{8}$$

in which the prime $'$ denotes $\partial/\partial n_x$, $r \equiv |s-x|$ is the distance between the source point s and collocation point x; n_i is the ith component of the outnormal vector at s; $\bar{n}_i$ is the ith component of the outnormal vector at x, as shown in Fig. 1, J_m and I_m denote the first kind of the mth order Bessel and modified Bessel functions,

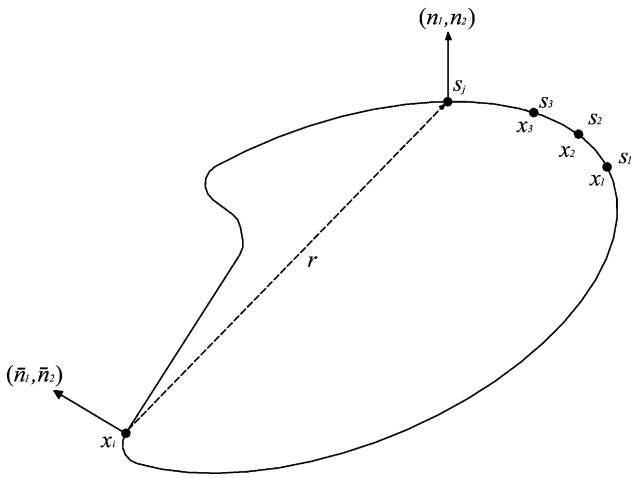

Fig. 1. Notations in the method of imaginary-part fundamental solution.

respectively, and $y_i \equiv s_i - x_i$, $i=1,2$, are the differences of the ith components of s and x, w and $\theta = \partial w/\partial n_x$ are the transverse deflection and its slope along the normal direction, respectively. It is noted that the differential formulae for the Bessel and modified Bessel functions have been utilized in deriving Eqs. (6)–(8), i.e.

$$J'_\ell(\lambda r) = -J_{\ell+1}(\lambda r) + \frac{\ell}{\lambda r} J_\ell(\lambda r), \quad \ell = 0,1,2,3,\ldots, \tag{9}$$

$$I'_\ell(\lambda r) = I_{\ell+1}(\lambda r) + \frac{\ell}{\lambda r} I_\ell(\lambda r), \quad \ell = 0,1,2,3,\ldots. \tag{10}$$

For simplicity, we consider the clamped plate with the following boundary conditions

$$w(x) = 0, \text{ and } \theta(x) = 0, \quad x \in B, \tag{11}$$

where B is the boundary. The main difference between the present formulation and the NDIF method proposed by Kang and Lee [36] is the choice of RBF. The NDIF method chose $W(s,x) = J_0(\lambda r)$ and $\Theta(s,x) = I_0(\lambda r)$. Although the selected RBF by Kang and Lee is simpler [36], it results in spurious eigenvalues which need special treatment. By matching the boundary conditions for x on the $2N$ boundary points into Eqs. (3) and (4), we have

$$\{0\} = [W]\{A\} + [\Theta]\{B\}, \tag{12}$$

$$\{0\} = [W']\{A\} + [\Theta']\{B\}, \tag{13}$$

where $\{A\}$ and $\{B\}$ are the vectors of undetermined coefficients, and $[W]$, $[\Theta]$, $[W']$ and $[\Theta']$ are influence matrices corresponding to the four kernels in Eqs. (5)–(8). The elements of the four matrices are shown below:

$$W_{ij} = W(s_j, x_i), \tag{14}$$

$$\Theta_{ij} = \Theta(s_j, x_i), \tag{15}$$

$$W'_{ij} = W'(s_j, x_i), \tag{16}$$

$$\Theta'_{ij} = \Theta'(s_j, x_i). \tag{17}$$

It is noted that the diagonal terms can be determined by the L'Hôspital's rule or invariant method. Although even number of nodes ($2N$) is considered here, odd number ($2N+1$) has also been implemented [44]. Eq. (12) can be rearranged to

$$\{A\} = -[W]^{-1}[\Theta]\{B\}. \tag{18}$$

By substituting Eq. (18) into Eq. (13), we have

$$-[W'][W]^{-1}[\Theta]\{B\} + [\Theta']\{B\} = \{0\}. \tag{19}$$

By collecting the terms of vector $\{B\}$ together, we obtain

$$[[\Theta'] - [W'][W]^{-1}[\Theta]]\{B\} = \{0\}) \Rightarrow [SM_N]\{B\} = \{0\}, \tag{20}$$

where

$$[SM_N] = [\Theta'] - [W'][W]^{-1}[\Theta]. \tag{21}$$

For the existence of non-trivial solution of $\{B\}$, the determinant of the matrix versus the eigenvalue must become zero, i.e.

$$\det[SM_N] = 0. \tag{22}$$

Although direct-searching eigenvalues is time consuming, it is no problem for computation of desk computer. For the generalized algebraic eigenproblem, some effective schemes have been proposed, e.g. William–Wellie algorithm [45]. Since this is not our main focus, the efficient algorithm was not discussed here.

3. Analytical study for the circular plate

3.1. Discrete system

For the circular case, we can express $x = (\rho, \phi)$ and $s = (R, \theta)$ in terms of polar coordinate. The four kernels can be expressed in terms of degenerate kernels as shown below [40],
where the subscripts 'I' and 'E' denote the interior ($R > \rho$) and exterior domains ($R < \rho$), respectively.

$$W(s,x) = \begin{cases} W_{\mathrm{I}}(\theta,\phi) = \dfrac{1}{8\lambda^2} \displaystyle\sum_{m=-\infty}^{\infty} [J_m(\lambda R)J_m(\lambda\rho) + (-1)^m I_m(\lambda R)I_m(\lambda\rho)]\cos(m(\theta-\phi)), & R > \rho \\ W_{\mathrm{E}}(\theta,\phi) = \dfrac{1}{8\lambda^2} \displaystyle\sum_{m=-\infty}^{\infty} [J_m(\lambda\rho)J_m(\lambda R) + (-1)^m I_m(\lambda\rho)I_m(\lambda R)]\cos(m(\theta-\phi)), & R < \rho \end{cases}, \tag{23}$$

$$\Theta(s,x)=\begin{cases}\Theta_{\mathrm{I}}(\theta,\phi)=\dfrac{1}{8\lambda}\displaystyle\sum_{m=-\infty}^{\infty}[J'_m(\lambda R)J_m(\lambda\rho)+(-1)^m I'_m(\lambda R)I_m(\lambda\rho)]\cos(m(\theta-\phi)), & R>\rho\\ \Theta_{\mathrm{E}}(\theta,\phi)=\dfrac{1}{8\lambda}\displaystyle\sum_{m=-\infty}^{\infty}[J_m(\lambda\rho)J'_m(\lambda R)+(-1)^m I_m(\lambda\rho)I'_m(\lambda R)]\cos(m(\theta-\phi)), & R<\rho\end{cases}, \tag{24}$$

$$W'(s,x)=\begin{cases}W'_{\mathrm{I}}(\theta,\phi)=\dfrac{1}{8\lambda}\displaystyle\sum_{m=-\infty}^{\infty}[J_m(\lambda R)J'_m(\lambda\rho)+(-1)^m I_m(\lambda R)I'_m(\lambda\rho)]\cos(m(\theta-\phi)), & R>\rho\\ W'_{\mathrm{E}}(\theta,\phi)=\dfrac{1}{8\lambda}\displaystyle\sum_{m=-\infty}^{\infty}[J'_m(\lambda\rho)J_m(\lambda R)+(-1)^m I'_m(\lambda\rho)I_m(\lambda R)]\cos(m(\theta-\phi)), & R<\rho\end{cases}, \tag{25}$$

$$\Theta'(s,x)=\begin{cases}\Theta'_{\mathrm{I}}(\theta,\phi)=\dfrac{1}{8}\displaystyle\sum_{m=-\infty}^{\infty}[J'_m(\lambda R)J'_m(\lambda\rho)+(-1)^m I'_m(\lambda R)I'_m(\lambda\rho)]\cos(m(\theta-\phi)), & R>\rho\\ \Theta'_{\mathrm{E}}(\theta,\phi)=\dfrac{1}{8}\displaystyle\sum_{m=-\infty}^{\infty}[J'_m(\lambda\rho)J'_m(\lambda R)+(-1)^m I'_m(\lambda\rho)I'_m(\lambda R)]\cos(m(\theta-\phi)), & R<\rho\end{cases}, \tag{26}$$

Since the rotation symmetry is preserved for a circular boundary, the four influence matrices in Eqs. (3) and (4) are denoted by $[W]$, $[\Theta]$, $[W']$ and $[\Theta']$ of the circulants with the elements

$$K_{ij}=K(R,\theta_j;\rho,\phi_i), \tag{27}$$

where the kernel K can be W, Θ, W' or Θ', ϕ_i and θ_j are the angles of observation and boundary points, respectively. By superimposing $2N$ lumped strength along the boundary, we have the influence matrices

$$[K]=\begin{bmatrix}a_0 & a_1 & a_2 & \cdots & a_{2N-2} & a_{2N-1}\\ a_{2N-1} & a_0 & a_1 & \cdots & a_{2N-3} & a_{2N-2}\\ a_{2N-2} & a_{2N-1} & a_0 & \cdots & a_{2N-4} & a_{2N-3}\\ \vdots & \vdots & \vdots & \ddots & \vdots & \vdots\\ a_1 & a_2 & a_3 & \cdots & a_{2N-1} & a_0\end{bmatrix}, \tag{28}$$

where the elements of the first row can be obtained by

$$a_{j-i}=K(s_j,x_i). \tag{29}$$

The matrix $[K]$ in Eq. (28) is found to be a circulant [25] since the rotational symmetry for the influence coefficients is considered. By introducing the following bases for the circulants, I, $(C_{2N})^1$, $(C_{2N})^2,\ldots$, and $(C_{2N})^{2N-1}$, we can expand $[K]$ into

$$[K]=a_0 I+a_1(C_{2N})^1+a_2(C_{2N})^2+\cdots+a_{2N-1}(C_{2N})^{2N-1}, \tag{30}$$

where I is a unit matrix and

$$C_{2N}=\begin{bmatrix}0&1&0&\cdots&0&0\\ 0&0&1&\cdots&0&0\\ \vdots&\vdots&\vdots&\ddots&\vdots&\vdots\\ 0&0&0&\cdots&0&1\\ 1&0&0&\cdots&0&0\end{bmatrix}_{2N\times 2N}. \tag{31}$$

Based on the circulant theory, the eigenvalues for the influence matrix, $[K]$, are found as follows

$$\lambda_\ell=a_0+a_1\alpha_\ell+a_2\alpha_\ell^2+\cdots+a_{2N-1}\alpha_\ell^{2N-1},\quad \ell=0,\pm1,\pm2,\ldots,\pm(N-1),N, \tag{32}$$

where λ_ℓ and α_ℓ are the eigenvalues for $[K]$ and $[C_{2N}]$, respectively. It is easily found that the eigenvalues for the circulant $[C_{2N}]$ are the roots for $\alpha^{2N}=1$ as shown below:

$$\alpha_\ell=\mathrm{e}^{\mathrm{i}(2\pi\ell/2N)},\quad \ell=0,\pm1,\pm2,\ldots,\pm(N-1),N \text{ or } \ell=0,1,2,\ldots,2N-1. \tag{33}$$

Substituting Eq. (33) into Eq. (32), we have

$$\lambda_\ell=\sum_{m=0}^{2N-1}a_m\alpha_\ell^m=\sum_{m=0}^{2N-1}a_m\mathrm{e}^{\mathrm{i}(2\pi/2N)m\ell},\quad \ell=0,\pm1,\pm2,\ldots,\pm(N-1),N. \tag{34}$$

According to the definition for a_m in Eq. (29), we have

$$a_m=a_{2N-m},\quad m=0,1,2,\ldots,2N-1. \tag{35}$$

Without loss of generality by setting $\phi=0$, substitution of Eq. (35) into Eq. (34) yields

$$\lambda_\ell = a_0 + (-1)^\ell a_N + \sum_{m=1}^{N-1} (\alpha_\ell^m + \alpha_\ell^{2N-m}) a_m$$

$$= \sum_{m=0}^{2N-1} \cos(m\ell\Delta\theta) a_m, \tag{36}$$

the Reimann sum of infinite terms reduces to the following integral

$$\lambda_\ell = \lim_{N\to\infty} \sum_{m=0}^{2N-1} \cos(m\ell\Delta\theta) W(m\Delta\theta, 0)$$

$$\approx \frac{1}{\rho\Delta\theta} \int_0^{2\pi} \cos(\ell\theta) W(\theta,0) \rho \mathrm{d}\theta, \tag{37}$$

where $\Delta\theta = 2\pi/2N$. By using the degenerate kernel for $W(s,x)$ in Eq. (23) and the orthogonal conditions, Eq. (37) reduces to ($\rho=R$)

$$\lambda_\ell = \frac{N}{4\lambda^2}[J_\ell(\lambda\rho)J_\ell(\lambda\rho) + (-1)^\ell I_\ell(\lambda\rho) I_\ell(\lambda\rho)],$$
$$\ell = 0, \pm 1, \pm 2, \ldots, \pm(N-1), N. \tag{38}$$

Similarly, we have

$$\mu_\ell = \frac{N}{4\lambda}[J_\ell(\lambda\rho)J'_\ell(\lambda\rho) + (-1)^\ell I_\ell(\lambda\rho) I'_\ell(\lambda\rho)],$$
$$\ell = 0, \pm 1, \pm 2, \ldots, \pm(N-1), N, \tag{39}$$

$$\nu_\ell = \frac{N}{4\lambda}[J'_\ell(\lambda\rho)J_\ell(\lambda\rho) + (-1)^\ell I'_\ell(\lambda\rho) I_\ell(\lambda\rho)],$$
$$\ell = 0, \pm 1, \pm 2, \ldots, \pm(N-1), N, \tag{40}$$

$$\delta_\ell = \frac{N}{4}[J'_\ell(\lambda\rho)J'_\ell(\lambda\rho) + (-1)^\ell I'_\ell(\lambda\rho) I'_\ell(\lambda\rho)],$$
$$\ell = 0, \pm 1, \pm 2, \ldots, \pm(N-1), N, \tag{41}$$

where μ_ℓ, ν_ℓ and δ_ℓ are the eigenvalues of $[\Theta]$, $[W']$ and $[\Theta']$ matrices, respectively. The determinants for the four matrices are obtained by multiplying all the eigenvalues as shown below:

$$\det[W] = \lambda_0(\lambda_1\lambda_2\cdots\lambda_{N-1})^2\lambda_N, \tag{42}$$

$$\det[\Theta] = \mu_0(\mu_1\mu_2\cdots\mu_{N-1})^2\mu_N, \tag{43}$$

$$\det[W'] = \nu_0(\nu_1\nu_2\cdots\nu_{N-1})^2\nu_N, \tag{44}$$

$$\det[\Theta'] = \delta_0(\delta_1\delta_2\cdots\delta_{N-1})^2\delta_N. \tag{45}$$

Since the four matrices $[W]$, $[\Theta]$, $[W']$ and $[\Theta']$ are all symmetric circulants, they can be expressed by

$$[W] = \Phi \begin{bmatrix} \lambda_0 & 0 & 0 & \cdots & 0 & 0 & 0 \\ 0 & \lambda_1 & 0 & \cdots & 0 & 0 & 0 \\ 0 & 0 & \lambda_{-1} & \cdots & 0 & 0 & 0 \\ \vdots & \vdots & \vdots & \ddots & \vdots & \vdots & \vdots \\ 0 & 0 & 0 & \cdots & \lambda_{(N-1)} & 0 & 0 \\ 0 & 0 & 0 & \cdots & 0 & \lambda_{-(N-1)} & 0 \\ 0 & 0 & 0 & \cdots & 0 & 0 & \lambda_N \end{bmatrix}_{2N\times 2N} \Phi^{-1}, \tag{46}$$

$$[\Theta] = \Phi \begin{bmatrix} \mu_0 & 0 & 0 & \cdots & 0 & 0 & 0 \\ 0 & \mu_1 & 0 & \cdots & 0 & 0 & 0 \\ 0 & 0 & \mu_{-1} & \cdots & 0 & 0 & 0 \\ \vdots & \vdots & \vdots & \ddots & \vdots & \vdots & \vdots \\ 0 & 0 & 0 & \cdots & \mu_{(N-1)} & 0 & 0 \\ 0 & 0 & 0 & \cdots & 0 & \mu_{-(N-1)} & 0 \\ 0 & 0 & 0 & \cdots & 0 & 0 & \mu_N \end{bmatrix}_{2N\times 2N} \Phi^{-1}, \tag{47}$$

$$[W'] = \Phi \begin{bmatrix} \nu_0 & 0 & 0 & \cdots & 0 & 0 & 0 \\ 0 & \nu_1 & 0 & \cdots & 0 & 0 & 0 \\ 0 & 0 & \nu_{-1} & \cdots & 0 & 0 & 0 \\ \vdots & \vdots & \vdots & \ddots & \vdots & \vdots & \vdots \\ 0 & 0 & 0 & \cdots & \nu_{(N-1)} & 0 & 0 \\ 0 & 0 & 0 & \cdots & 0 & \nu_{-(N-1)} & 0 \\ 0 & 0 & 0 & \cdots & 0 & 0 & \nu_N \end{bmatrix}_{2N\times 2N} \Phi^{-1}, \tag{48}$$

$$[\Theta'] = \Phi \begin{bmatrix} \delta_0 & 0 & 0 & \cdots & 0 & 0 & 0 \\ 0 & \delta_1 & 0 & \cdots & 0 & 0 & 0 \\ 0 & 0 & \delta_{-1} & \cdots & 0 & 0 & 0 \\ \vdots & \vdots & \vdots & \ddots & \vdots & \vdots & \vdots \\ 0 & 0 & 0 & \cdots & \delta_{(N-1)} & 0 & 0 \\ 0 & 0 & 0 & \cdots & 0 & \delta_{-(N-1)} & 0 \\ 0 & 0 & 0 & \cdots & 0 & 0 & \delta_N \end{bmatrix}_{2N\times 2N} \Phi^{-1}, \tag{49}$$

where

$$\Phi = \frac{1}{\sqrt{2N}} \times \begin{bmatrix} 1 & 1 & 0 & \cdots & 1 & 0 & 1 \\ 1 & \cos\left(\frac{2\pi}{2N}\right) & \sin\left(\frac{2\pi}{2N}\right) & \cdots & \cos\left(\frac{2\pi(N-1)}{2N}\right) & \sin\left(\frac{2\pi(N-1)}{2N}\right) & \cos\left(\frac{2\pi N}{2N}\right) \\ 1 & \cos\left(\frac{4\pi}{2N}\right) & \sin\left(\frac{4\pi}{2N}\right) & \cdots & \cos\left(\frac{4\pi(N-1)}{2N}\right) & \sin\left(\frac{4\pi(N-1)}{2N}\right) & \cos\left(\frac{4\pi N}{2N}\right) \\ \vdots & \vdots & \vdots & \ddots & \vdots & \vdots & \vdots \\ 1 & \cos\left(\frac{2\pi(2N-2)}{2N}\right) & \sin\left(\frac{2\pi(2N-2)}{2N}\right) & \cdots & \cos\left(\frac{\pi(4N-4)(N-1)}{2N}\right) & \sin\left(\frac{\pi(4N-4)(N-1)}{2N}\right) & \cos\left(\frac{\pi(4N-4)(N)}{2N}\right) \\ 1 & \cos\left(\frac{2\pi(2N-1)}{2N}\right) & \sin\left(\frac{2\pi(2N-1)}{2N}\right) & \cdots & \cos\left(\frac{\pi(4N-2)(N-1)}{2N}\right) & \sin\left(\frac{\pi(4N-2)(N-1)}{2N}\right) & \cos\left(\frac{\pi(4N-2)(N)}{2N}\right) \end{bmatrix}_{2N\times 2N}. \tag{50}$$

By employing Eqs. (46)–(49) for Eq. (21), we have

$$[SM_N] = \Phi \begin{bmatrix} \sigma_0 & 0 & 0 & \cdots & 0 & 0 & 0 \\ 0 & \sigma_1 & 0 & \cdots & 0 & 0 & 0 \\ 0 & 0 & \sigma_{-1} & \cdots & 0 & 0 & 0 \\ \vdots & \vdots & \vdots & \ddots & \vdots & \vdots & \vdots \\ 0 & 0 & 0 & \cdots & \sigma_{(N-1)} & 0 & 0 \\ 0 & 0 & 0 & \cdots & 0 & \sigma_{-(N-1)} & 0 \\ 0 & 0 & 0 & \cdots & 0 & 0 & \sigma_N \end{bmatrix} \Phi^{-1}, \tag{51}$$

where

$$\sigma_\ell = \frac{N}{4} \frac{[J'_\ell(\lambda\rho)I_\ell(\lambda\rho) - I'_\ell(\lambda\rho)J_\ell(\lambda\rho)]^2}{J_\ell(\lambda\rho)J_\ell(\lambda\rho) + (-1)^\ell I_\ell(\lambda\rho)I_\ell(\lambda\rho)}, \tag{52}$$

$\ell = 0, \pm 1, \pm 2, \ldots, \pm(N-1), N.$

According to Eqs. (51) and (52), we have

$$\det[SM_N] = \det|\Phi|\sigma_0(\sigma_1\sigma_2\cdots\sigma_{N-1})^2\sigma_N\det|\Phi^{-1}| = \sigma_0(\sigma_1\sigma_2\cdots\sigma_{N-1})^2\sigma_N, \tag{53}$$

since $\det|\Phi| = \det|\Phi^{-1}| = 1$. By employing the differential formulae for the Bessel and the modified Bessel functions as shown below

$$J'_\ell(\lambda\rho) = \frac{J_{\ell-1}(\lambda\rho) - J_{\ell+1}(\lambda\rho)}{2}, \quad \ell = 0,1,2,3,\ldots, \tag{54}$$

$$I'_\ell(\lambda\rho) = \frac{I_{\ell-1}(\lambda\rho) + I_{\ell+1}(\lambda\rho)}{2}, \quad \ell = 0,1,2,3,\ldots, \tag{55}$$

we obtain the following identity for any λ

$$J'_\ell(\lambda\rho)I_\ell(\lambda\rho) - I'_\ell(\lambda\rho)J_\ell(\lambda\rho) = -[J_\ell(\lambda\rho)I_{\ell+1}(\lambda\rho) + I_\ell(\lambda\rho)J_{\ell+1}(\lambda\rho)]. \tag{56}$$

Zero determinant in Eq. (53) implies that the eigenequation is

$$\frac{[J_\ell(\lambda\rho)I_{\ell+1}(\lambda\rho) + I_\ell(\lambda\rho)J_{\ell+1}(\lambda\rho)]^2}{J_\ell(\lambda\rho)J_\ell(\lambda\rho) + (-1)^\ell I_\ell(\lambda\rho)I_\ell(\lambda\rho)} = 0, \tag{57}$$

$\ell = 0, \pm 1, \pm 2, \ldots, \pm(N-1), N.$

Since the denominator term of $J_\ell(\lambda\rho)J_\ell(\lambda\rho) + (-1)^\ell I_\ell(\lambda\rho)I_\ell(\lambda\rho)$ is never zero for any positive value of λ, the eigenequation in Eq. (57) reduces to

$$[J_\ell(\lambda\rho)I_{\ell+1}(\lambda\rho) + I_\ell(\lambda\rho)J_{\ell+1}(\lambda\rho)]^2 = 0, \tag{58}$$

$\ell = 0, \pm 1, \pm 2, \ldots, \pm(N-1), N.$

After comparing with the exact solution for the clamped circular plate, we find that the true eigenequation is $J_\ell(\lambda\rho)I_{\ell+1}(\lambda\rho) + I_\ell(\lambda\rho)J_{\ell+1}(\lambda\rho) = 0$, $\ell = 0, \pm 1, \pm 2, \ldots, \pm(N-1), N$, for plate vibration. In another words, the exact eigensolution for a continuous system can be obtained by approaching N in the discrete system to infinity. Once the eigenvalue λ is obtained, we can determine the non-trivial vector $\{B\}$. Since $[W]$ in Eq. (42) is never singular due to non-zero eigenvalues in Eq. (38), $\{A\}$ can be obtained using Eq. (18). Therefore, the interior mode can be calculated by using Eq. (3). Instead of appearing the spurious eigenvalues in the Kang and Lee method [36], contamination of spurious eigenvalues are not present in our approach.

3.2. Continuous system

For the purpose of analytical study, we use the continuous system to obtain the eigenequation. The unknowns densities $A(s)$ and $B(s)$, can be expanded into Fourier series by

$$A(s) = a_0 + \sum_{n=1}^{\infty} (a_n \cos(n\theta) + b_n \sin(n\theta)), \qquad s \in B, \tag{59}$$

$$B(s) = p_0 + \sum_{n=1}^{\infty} (p_n \cos(n\theta) + q_n \sin(n\theta)), \qquad s \in B, \tag{60}$$

where a_n, b_n, p_n and q_n are the undetermined Fourier coefficients. For the clamped boundary conditions, $w = 0$ and $\theta = 0$, we have

$$0 = \int_0^{2\pi} W_{\mathrm{E}}(s,x)\left(a_0 + \sum_{n=1}^{\infty}(a_n\cos(n\theta) + b_n\sin(n\theta))\right)\rho \mathrm{d}\theta + \int_0^{2\pi} \Theta_{\mathrm{E}}(s,x)\left(p_0 + \sum_{n=1}^{\infty}(p_n\cos(n\theta) + q_n\sin(n\theta))\right)\rho \mathrm{d}\theta, \quad x \in B, \tag{61}$$

$$0 = \int_0^{2\pi} W'_{\mathrm{E}}(s,x)\left(a_0 + \sum_{n=1}^{\infty}(a_n\cos(n\theta) + b_n\sin(n\theta))\right)\rho \mathrm{d}\theta + \int_0^{2\pi} \Theta'_{\mathrm{E}}(s,x)\left(p_0 + \sum_{n=1}^{\infty}(p_n\cos(n\theta) + q_n\sin(n\theta))\right)\rho \mathrm{d}\theta, \quad x \in B. \tag{62}$$

By substituting the degenerate kernels of Eqs. (23) and (24) into Eq. (61) and employing the orthogonality condition of the Fourier series, the Fourier coefficients a_n, b_n, p_n and q_n satisfy

$$p_n = -\frac{1}{\lambda}\frac{J_n(\lambda\rho)J_n(\lambda\rho) + (-1)^n I_n(\lambda\rho)I_n(\lambda\rho)}{J'_n(\lambda\rho)J_n(\lambda\rho) + (-1)^n I'_n(\lambda\rho)I_n(\lambda\rho)}a_n, \quad n = 0,1,2,\ldots, \tag{63}$$

$$q_n = -\frac{1}{\lambda}\frac{J_n(\lambda\rho)J_n(\lambda\rho) + (-1)^n I_n(\lambda\rho)I_n(\lambda\rho)}{J'_n(\lambda\rho)J_n(\lambda\rho) + (-1)^n I'_n(\lambda\rho)I_n(\lambda\rho)}b_n, \quad n = 0,1,2,\ldots. \tag{64}$$

Similarly Eq. (62) yields

$$p_n = -\frac{1}{\lambda}\frac{J'_n(\lambda\rho)J_n(\lambda\rho) + (-1)^n I'_n(\lambda\rho)I_n(\lambda\rho)}{J'_n(\lambda\rho)J'_n(\lambda\rho) + (-1)^n I'_n(\lambda\rho)I'_n(\lambda\rho)}a_n, \quad n = 0,1,2,\ldots, \tag{65}$$

$$q_n = -\frac{1}{\lambda}\frac{J'_n(\lambda\rho)J_n(\lambda\rho) + (-1)^n I'_n(\lambda\rho)I_n(\lambda\rho)}{J'_n(\lambda\rho)J'_n(\lambda\rho) + (-1)^n I'_n(\lambda\rho)I'_n(\lambda\rho)}b_n, \quad n = 0,1,2,\ldots. \tag{66}$$

To seek non-trivial data for the generalized coefficients of a_n, p_n, b_n and q_n, we can obtain the eigenequations by either from Eqs. (63) and (65) or from Eqs. (64) and (66)

$$(J'_n(\lambda\rho)I_n(\lambda\rho) - I'_n(\lambda\rho)J_n(\lambda\rho))^2 = (J_n(\lambda\rho)I_{n+1}(\lambda\rho) + I_n(\lambda\rho)J_{n+1}(\lambda\rho))^2 = 0. \tag{67}$$

The eigenequation in Eq. (67) is the same with Eq. (52) obtained by using circulants in the discrete system.

3.3. Derivation of the eigenmode

By substituting the degenerate kernels of Eqs. (23)–(26) for the interior point ($0 < r < \rho$) and the relationships of Eqs. (63)–(66) between generalized coefficients of $A(s)$ and $B(s)$ into Eq. (2), we have

$$w(r,\phi) = (J_n(\lambda\rho)I_{n+1}(\lambda\rho) + I_n(\lambda\rho)J_{n+1}(\lambda\rho)) \times (-1)^n \frac{(J_n(\lambda r)I_n(\lambda\rho) - I_n(\lambda r)J_n(\lambda\rho))}{(J_n(\lambda\rho)J'_n(\lambda\rho) + (-1)^n I_n(\lambda\rho)I'_n(\lambda\rho))} \times (a_n\cos(n\phi) + b_n\sin(n\phi)), \quad n = 1,2,3,\ldots, \quad 0 < r < \rho, \quad 0 \le \phi < 2\pi. \tag{68}$$

It is interesting to find that the eigenequation of Eq. (58) is imbedded in Eq. (68). Theoretically speaking, the interior mode is a null field when λ is an eigenvalue. However, the interior mode with clear nodal lines can be found since no true zero can be obtained in real calculations.

4. Calculation of eigenvalues, boundary modes and interior modes using the SVD technique

In order to obtain the eigenvalues λ and boundary modes $\{A\}$ and $\{B\}$ at the same time, we employ the SVD technique to decompose $[SM_N]$ matrix into

$$[SM_N] = \Phi\Sigma\Psi^{\mathrm{T}}, \tag{69}$$

where Φ and Ψ are left and right unitary matrices, and Σ is a matrix with diagonal terms composed of singular values [46]. The analytical form of Eq. (69) is shown in Eq. (51). By detecting the minimum singular value to be zero versus λ, we obtain the eigenvalues by employing the direct searching scheme. In the meanwhile, the non-zero boundary mode for $\{B\}$ is extracted from the corresponding right unitary vector with the zero singular value in Ψ since

$$[SM_N]\{B\} = \{0\}. \tag{70}$$

By substituting the boundary mode $\{B\}$ into Eq. (18), the vector of $\{A\}$ can be directly determined since $[W]^{-1}$ exists as shown in the circular case. After the vectors $\{A\}$ and $\{B\}$ are determined, the interior mode can be obtained by using Eq. (3). In summary, the flow chart for the present method is shown in Fig. 2.

5. Numerical results and discussions

Case 1: Circular plate (clamped boundary)

A circular plate with a radius ($\rho = 1$ m) subjected to the clamped boundary condition ($w = 0$ and $\partial w/\partial n = 0$) is considered. In this case, analytical solutions of eigenequation and eigenmode are shown in Eqs. (67) and (68).

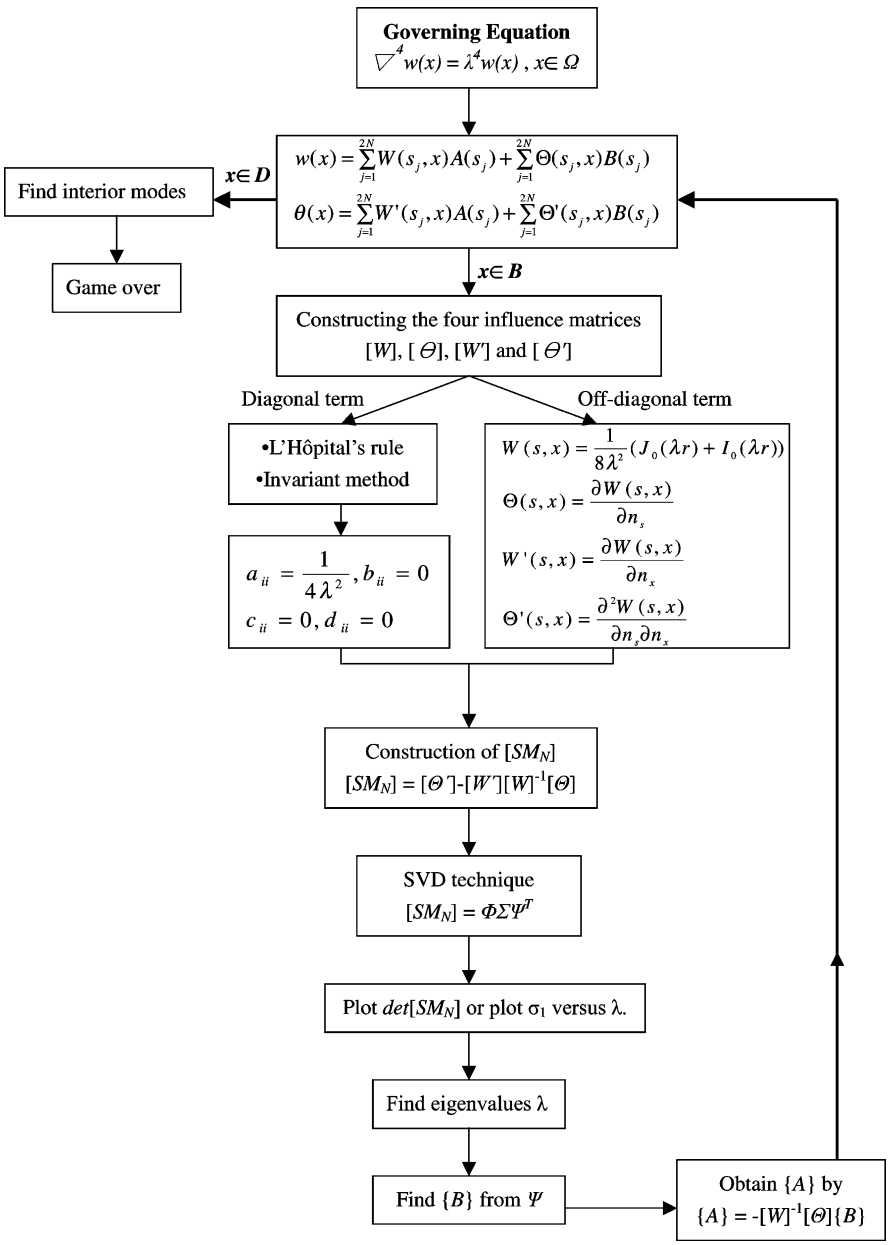

Fig. 2. Flow chart of the present method.

By collocating 18 nodes on the circular boundary, the results by using the imaginary-part kernel are obtained as shown in Table 1 for the eigenvalues in comparison with other approaches. Good agreement is made. Fig. 3(a) shows the minimum singular value versus λ. To compare with Kang and Lee's results, Fig. 3(b) shows the determinant of $[SM_N]$ versus λ using the present method in comparison with the circulant methods and Kang and Lee results [36]. The former six eigenvalues are obtained as shown in Table 1 by considering the near zero determinant or near zero singular value. The eigenvalues agree well with the analytical solution.

Case 2: Rectangular plate (clamped boundary)

A rectangular plate with dimensions 1.2 m × 0.9 m subjected to the clamped boundary condition ($w = 0$ and $\partial w/\partial n = 0$) is considered. In this case, the analytical solution is not available. The Kang and Lee results and FEM [36] using ANSYS are compared with.

Table 1
The former six eigenvalues for the clamped circular plate using different approaches

	λ_1	λ_2	λ_3	λ_4	λ_5	λ_6
NASA SP-160	3.196	4.611	5.906	6.306	7.144	7.799
Integral Eq.	3.2	4.6	5.9	6.3	7.2	7.9
Kang and Lee	3.196	4.611	5.906	6.306	7.144	7.799
Circulant method	3.20	4.61	5.91	6.31	7.14	7.80
Present method	3.195	4.611	5.906	6.306	7.143	7.798
Exact solution	3.196	4.611	5.906	6.306	7.144	7.799

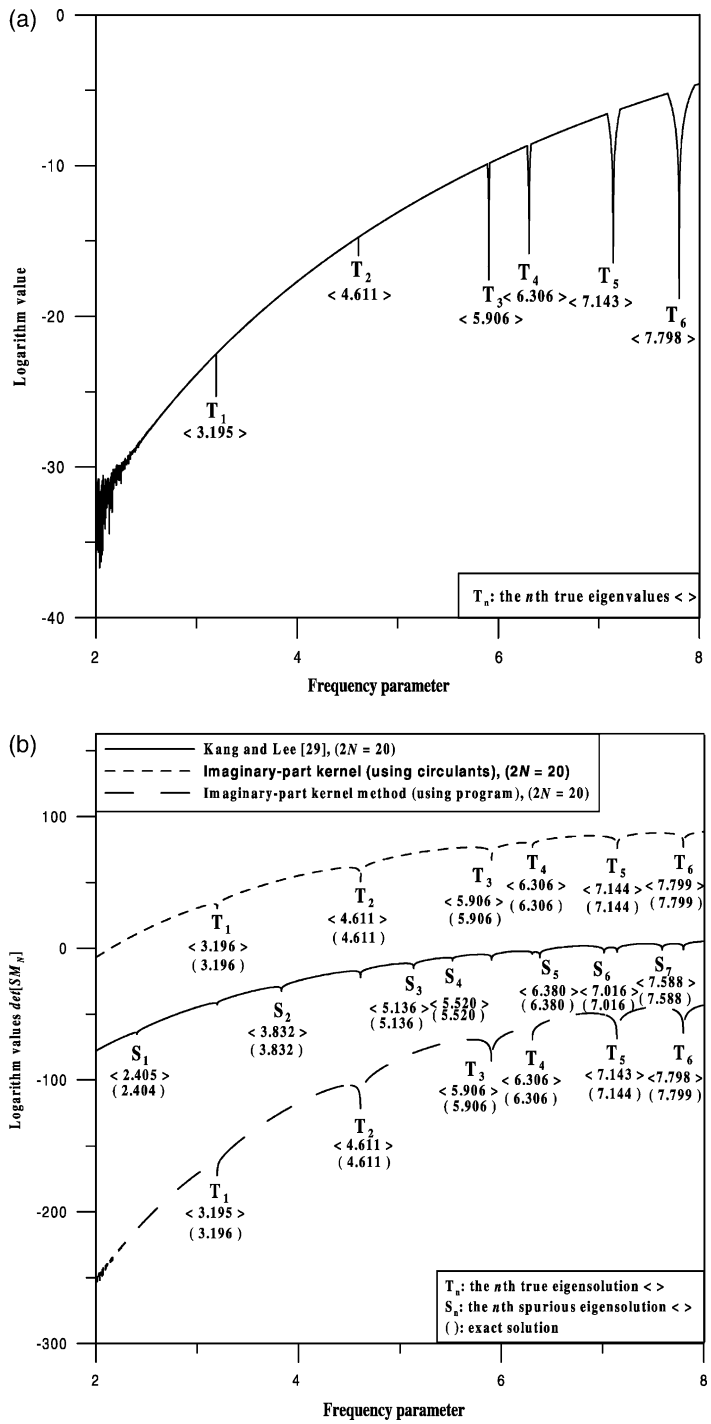

Fig. 3. (a) Logarithm curve for the minimum singular value versus frequency parameter using the present method. (b) Logarithm curve for det$[SM_N]$ versus frequency parameter of the circular clamped plate using the different methods.

Since the normal vector on the boundary is concerned, the double notes at the corner are discretized. By collocating 12 nodes on the boundary, the results are obtained as shown in Table 2 [47] for the eigenvalues in comparison with those of other approaches. Good agreement is obtained. Fig. 4 shows the minimum singular value of $[SM_N]$ versus λ using the present approach. The former six eigenvalues are obtained as shown in Fig. 4.

Table 2
The former six eigenvalues for the clamped rectangular plate using different approaches

	λ_1	λ_2	λ_3	λ_4	λ_5	λ_6
Dickinson [38]	5.964	7.730	9.151	9.975	10.30	11.99
ANSYS (441 nodes)	5.946	7.701	9.114	9.938	10.24	11.91
ANSYS (961 nodes)	5.950	7.706	9.123	9.948	10.26	11.94
Present method	5.952	7.703	9.129	9.947	10.266	11.95
Kang and Lee	5.952	7.703	9.131	9.955	10.27	11.95

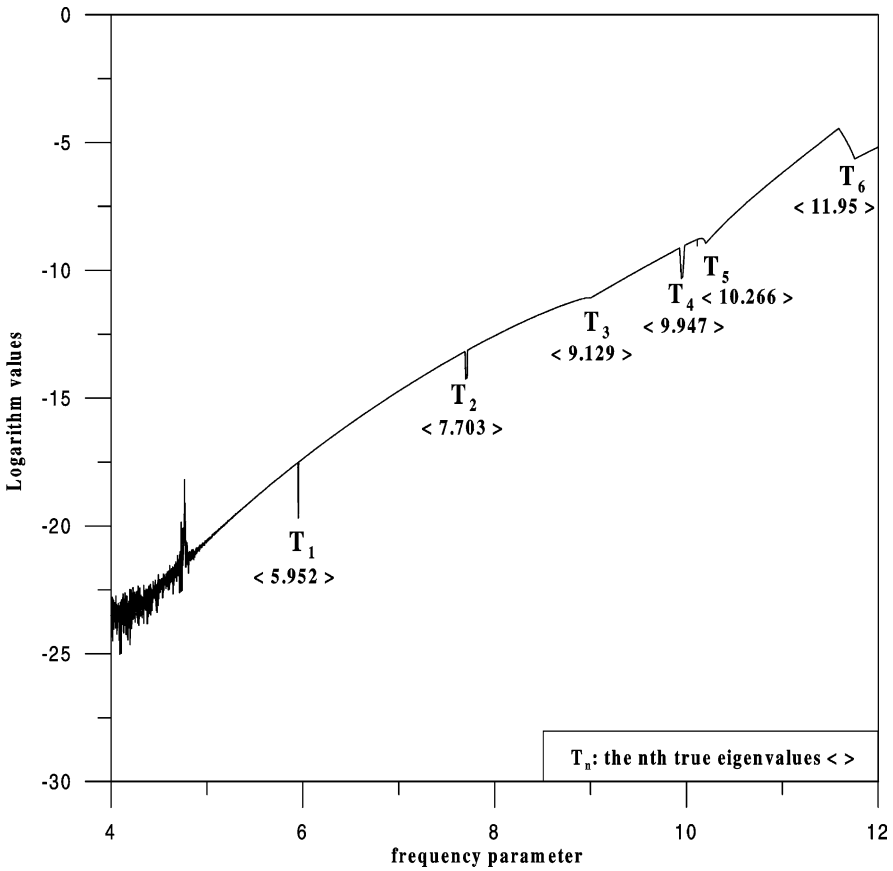

Fig. 4. Logarithm curve for the minimum singular value versus frequency parameter of the rectangular clamped plate using the present method.

6. Conclusions

We have developed a meshless method for the plate vibration problem with a clamped boundary condition by using the imaginary-part fundamental solution, which was chosen as a RBF to approximate the solution. Neither boundary elements nor singularities are required. Free of introducing the fictitious boundary, no singularity is encountered. Instead of appearing the spurious eigenvalues in the NDIF method, the present method is free of spurious eigenvalues. For a circular plate, the eigenvalue, boundary mode and interior mode were derived analytically by using the degenerate kernel, Fourier series and circulants. Although the circular case lacks generality, it lends significant insight into the occurring mechanism of spurious eigensolution. Therefore, we chose the circular cases to verify our approach in the continuous and discrete systems. The scheme for the circular plate can be extended to the general situations, e.g. rectangular clamped plates and circular plates subject to the simply supported boundary conditions [48]. The general cases were numerically demonstrated to check the validity of the meshless formulation.

Acknowledgements

Financial support from the National Science Council under Grant No. NSC-90-2211-E-019-006 for National Taiwan Ocean University is gratefully acknowledged.

References

[1] Gingold RA, Maraghan JJ. Smoothed particle hydrodynamics: theory and applications to non-spherical stars. Monthly Notices of the Royal Astronomical Society 1977;181:375–89.
[2] Belystcho T, Lu Y, Gu L. Element free Galerkin methods. Int J Numer Meth Engng 1994;37:229–56.
[3] Liu WK, Jun S, Zhang YF. Reproducing kernel particle methods. Int J Numer Meth Engng 1995;20:1081–1106.
[4] Mukherjee YX, Mukherjee S. The boundary node method for potential problems. Int J Numer Meth Engng 1997;40:797–815.
[5] Atluri SN, Zhu T. A new meshless local Petrov–Galerkin (MLPG) approach in computational mechanics. Comput Mech 1998;22:117–27.
[6] Sladek V, Sladek J, Atluri SN, Van Keer R. Numerical integration of singularities in meshless implementation of local boundary integral equations. Comput Mech 2000;25:394–403.
[7] Chen CS, Rashed YF, Golberg MA. A mesh-free method for linear diffusion equations. Numer Heat Transfer, Part B 1998;33:469–86.

[8] Golberg MA, Chen CS, Ganesh M. Particular solutions of 3D Helmholtz-type equations using compactly supported radial basis functions. Engng Anal Bound Elem 2000;24:539–47.
[9] Zhang X, Song KZ, Lu MW, Liu X. Meshless methods based on collocation with radial basis functions. Comput Mech 2000;26: 333–43.
[10] Chen W, Tanaka M. Relationship between boundary integral equation and radial basis function. Invited talk to the 52th Symposium of Japan Society for Computational Methods in Engineering (JASCOME) on BEM, Tokyo; 2000.
[11] Chen W, Tanaka M. A meshless, exponential convergence, integration-free, and boundary-only RBF technique. Comput Math Appl 2002;43:379–91.
[12] Chen W. New RBF collocation schemes and dernel RBFs with applications. Lecture Notes in Computational Science and Engineering 2002;26:73–84.
[13] Chen W. Meshfree boundary particle method applied to Helmholtz problems. Engng Anal Bound Elem 2002;26(7):557–81.
[14] Chen W. Symmetric boundary knot method. Engng Anal Bound Elem 2002;26(6):489–94.
[15] Chen W, Tanaka M. New insights into boundary-only and domain-type RBF methods. Int J Nonlinear Sci Numer Simul 2000;1(3):145–51.
[16] Hon YC, Chen W. Boundary knot method for 2D and 3D Helmholtz and convection–diffusion problems under complicated geometry. Int J Numer Meth Engng 2003;56:1931–48.
[17] Kamiya N, Ando E, Nogae K. A new complex-valued formulation and eigenvalue analysis of the Helmholtz equation by boundary element method. Adv Engng Software 1996;26:219–27.
[18] Yeih W, Chen JT, Chen KH, Wong FC. A study on the multiple reciprocity method and complex-valued formulation for the Helmholtz equation. Adv Engng Software 1998;29(1):7–12.
[19] Agnantiaris JP, Beskos DE. Some studies on dual reciprocity BEM for elastodynamic analysis. Comput Mech 1996;17:207–77.
[20] Banerjee PK, Ahmad S, Wang HC. A new BEM formulation for the acoustic eigen-frequency analysis. Int J Numer Meth Engng 1998;26: 1299–309.
[21] Chen JT, Wong FC. Analytical derivations for one-dimensional eigenproblems using dual BEM and MRM. Engng Anal Bound Elem 1997;20(1):25–33.
[22] Chen JT, Wong FC. Dual formulation of multiple reciprocity method for the acoustic mode of a cavity with a thin partition. J Sound Vibr 1998;217:75–95.
[23] Nowak AJ, Neves AC, editors. Multiple reciprocity boundary element method. Southampton: Computational Mechanics Publication; 1994.
[24] Chen JT, Huang CX, Chen KH. Determination of spurious eigenvalues and multiplicities of true eigenvalues using the real-part dual BEM. Comput Mech 1999;24(1):41–51.
[25] Kuo SR, Chen JT, Huang CX. Analytical study and numerical experiments for true and spurious eigensolutions of a circular cavity using the real-part dual BEM. Int J Numer Meth Engng 2000;48: 1401–22.
[26] Chen JT, Kuo SR, Chen KH. A nonsingular integral formulation for the Helmholtz eigenproblems of a circular domain. J Chin Inst Engrs 1999;22(6):729–39.
[27] Tai GRG, Shaw RP. Helmholtz equation eigenvalues and eigenmodes for arbitrary domains. J Acoust Soc Am 1974;56:796–804.
[28] Kamiya N, Andoh E. A note on multiple reciprocity integral formulation for the Helmholtz equation. Commun Numer Meth Engng 1993;9:9–13.
[29] De Mey G. A simplified integral equation method for the calculation of the eigenvalues of Helmholtz equation. J Acoust Soc Am 1977;11: 1340–2.
[30] Beskos DE. Boundary element methods in dynamic analysis. Appl Mech Rev 1987;40(1):1–23.
[31] Beskos DE. Boundary element methods in dynamic analysis. Appl Mech Rev, Part II (1986–1996) 1997;50(3):149–97.
[32] Beskos DE. Boundary element analysis of plates and shells. Berlin: Springer; 1991.
[33] Kang SW, Lee JM, Kang YJ. Vibration analysis of arbitrary shaped membranes using non-dimensional dynamic influence function. J Sound Vibr 1999;221(1):117–32.
[34] Kang SW, Lee JM. Application of free vibration analysis of membranes using the non-dimensional dynamic influence function. J Sound Vibr 2000;234(3):455–70.
[35] Kang SW, Lee JM. Eigenmode analysis of arbitrarily shaped two-dimensional cavities by the method of point matching. J Acoust Soc Am 2000;107(3):1153–60.
[36] Kang SW, Lee JM. Free vibration analysis of arbitrary shaped plates with clamped edges using wave-type functions. J Sound Vibr 2001; 242(1):9–26.
[37] Chen JT, Kuo SR, Chen KH, Cheng YC. Comments on vibration analysis of arbitrary shaped membranes using non-dimensional dynamic influence function. J Sound Vibr 2000;235(1):156–71.
[38] Chen JT, Chang MH, Chung IL, Cheng YC. Comments on eigenmode analysis of arbitrarily shaped two-dimensional cavities by the method of point matching. J Acoust Soc Am 2002;111(1):33–6.
[39] Chen JT, Chen IL, Chen KH, Lee YT. Comment on free vibration analysis of arbitrarily shaped plates with clamped edges using wave-type function. J Sound Vibr 2003;262(2):370–78.
[40] Chen JT, Chang MH, Chen KH, Lin SR. The boundary collocation method with meshless concept for acoustic eigenanalysis of two-dimensional cavities using radial basis function. J Sound Vibr 2002; 257(4):667–711.
[41] Chen JT, Chang MH, Chen KH, Chen IL. Boundary collocation method for acoustic eigenanalysis of three-dimensional cavities using radial basis function. Comput Mech 2002;29:392–408.
[42] Goldberg JL. Matrix theory with applications. New York: McGraw-Hill; 1991.
[43] Kitahara M. Boundary integral equation methods in eigenvalue problems of elasto-dynamics and thin plates. Amsterdam: Elsevier; 1985.
[44] Chen JT, Chiu YP. On the pseudo-differential operators in the dual boundary integral equations using degenerate kernels and circulants. Engng Anal Bound Elem 2002;26(1):41–53.
[45] Williams FW, Wittrick WH. An automatic computational procedure for calculating natural frequencies of skeletal structures. Int J Mech Sci 1970;12(9):781–91.
[46] Golub GH, Van Loan CF. Matrix computations, 2nd ed. Baltimore: The Johns Hopkins University Press; 1989.
[47] Dickinson SM. The buckling and frequency of flexural vibration of rectangular, isotropic and orthotropic plates using Rayleigh's method. J Sound Vibr 1978;61:1–8.
[48] Lee YT, Chen IL, Chen KH, Chen JT. A new meshless method for free vibration analysis of plates using radial basis function. The 26th National Conference on Theoretical and Applied Mechanics, Taiwan, ROC; 2002.